Optimizing Hydrothermal Temperature for Ni-Based OER Catalysts

Elham Khorashadizade[1*] and Elahe Fattahy Ardakani[1,2]

[1]Pasargad Institute for Advanced Innovative Solutions (PIAIS), Tehran, Iran 1991633361
[2]Department of Converging Technologies, Khatam University, Tehran, Iran 19916-33357
Elham.khorashadizade@piais.ir

Abstract. Advancing electrochemical water splitting for sustainable hydrogen production depends on the development of robust and efficient oxygen evolution reaction (OER) electrocatalysts. Nickel-based materials, such as nickel hydroxide (Ni $(OH)_2$) and nickel oxyhydroxide (NiOOH), are attractive candidates for OER in alkaline environments due to their affordability and favorable redox characteristics. However, the effect of hydrothermal synthesis temperature on their structure and catalytic performance has not been fully clarified. In this study, we fabricated $Ni(OH)_2$/NiOOH thin films on nickel foam using hydrothermal synthesis at temperatures ranging from 120 °C to 180 °C. The fabricated thin films were evaluated using field emission electron microscopy, linear sweep voltammetry, Tafel analysis, and measurements of double-layer capacitance (C_{dl}) and electrochemical surface area (ECSA). Our results show that both catalytic activity and surface properties are highly sensitive to hydrothermal temperature, with the film produced at 160 °C displaying the best OER performance as well as the highest C_{dl} and ECSA values. These findings highlight the importance of optimizing hydrothermal temperature to control the microstructure and active site density of Ni $(OH)_2$/NiOOH films, identifying 160 °C as the most effective condition for enhancing catalytic activity in alkaline water splitting.

Keywords: Oxygen Evolution Reaction (OER), Hydrothermal Synthesis, Electrocatalysis, Nickel-based electrodes.

1 Introduction

The increasing demand for sustainable and carbon-neutral energy sources has made electrochemical water splitting a key area of research for hydrogen and oxygen production. One of the main obstacles in this process is the oxygen evolution reaction (OER), which is slow due to its complex four-electron transfer and the need for a high overpotential [1,2]. To make water electrolysis more practical, it is important to develop electrocatalysts that are both efficient and stable, using materials that are abundant and cost-effective, especially for alkaline environments [3,4]. Nickel-based compounds, such as nickel hydroxide ($Ni(OH)_2$) and nickel oxyhydroxide (NiOOH), are promising candidates because of their low cost, good redox properties, and strong

R. Rzayev et al. (eds.), *Proceedings of the International Conference on Current Problems in Engineering and Applied Sciences (ICCPEAS 2025)*, Advances in Engineering Research 299,
https://doi.org/10.2991/978-94-6239-668-5_23

performance in alkaline media [5,6]. However, their effectiveness depends on several factors, including crystal structure, surface area, conductivity, and the manner in which they interact with their supporting materials [7,8].

Hydrothermal synthesis is a practical and scalable method for preparing nanostructured $Ni(OH)_2$/NiOOH films directly on conductive substrates like nickel foam, which offers a high surface area and excellent conductivity [9]. While previous studies have mainly focused on changing catalyst loading, adding dopants, or making composites [10,11], there is still limited understanding of how synthesis conditions, especially synthesis temperature, affect the structure and electrochemical characteristic of these films. In this work, we systematically study the effect of hydrothermal temperature on the growth, structure, and OER activity of $Ni(OH)_2$/NiOOH thin films on nickel foam. Through the application of methods like cyclic voltammetry, linear sweep voltammetry, and Tafel analysis, we elucidate the impact of temperature on the connection between structure and catalytic efficiency, offering a clear strategy for enhancing nickel-based catalysts for alkaline water oxidation [12,13].

2 Materials and Method

2.1 Fabrication of Ni-Based Electrodes

All chemicals used were of analytical grade and were applied without any additional purification. Four pieces of nickel foam, each approximately 1.0 cm × 3.0 cm in size, were prepared to serve as both the hydrothermal precursor and substrate. These pieces were cleaned ultrasonically in acetone, absolute ethanol, and deionized water each for 15 minutes. After cleaning, the nickel foams were immersed into 40 ml deionized water in a Teflon-lined stainless-steel autoclave (50 ml) and heated at 120, 140, 160, and 180 °C for 24 hours (Fig.1). Then they were washed with distilled water carefully and dried at 60 °C for 2 hours. The resulted thin films hydrothermally treated at 120, 140, 160, and 180 °C were labeled as H-120, H-140, H-160, and H-180, respectively.

2.2 Characterization

The surface morphology of the prepared samples was analyzed using a field-emission scanning electron microscope (FE-SEM, TESCAN, MIRA 3 LMU). Fourier-transform infrared (FTIR) spectroscopy was performed using a high-resolution FTIR spectrometer equipped with an attenuated total reflectance (ATR) module. Spectra were collected in the wavenumber range of 400–4000 cm^{-1} with a resolution of 4 cm^{-1}, and each spectrum represents the average of 32 scans to ensure a high signal-to-noise ratio. All electrochemical measurements were performed using an Autolab (PGTAT302) in a conventional three-electrode cell. The resulted thin films served as the working electrode (1 cm^2), platinum acted as the counter electrode, and Ag/AgCl was used as the reference electrode in a 1 M potassium hydroxide aqueous solution (KOH). The potentials presented in this study were calibrated to the RHE using the following equation [14]:

$$E(RHE) = E(Ag/AgCl) + (0.197\ V) + 0.059\ pH \quad (1)$$

The linear sweep voltammetry (LSV) was conducted within a voltage range of 1.0 to 2.8 V (vs. RHE) at a scanning rate of 5.0 mV/s, without any prior activation process before the polarization curves were recorded. Additionally, the LSV curves were not subjected to iR correction. When calculating the current density, the working surface area was determined from one side only. Moreover, electrochemically active surface areas (ECSAs) can be estimated from the electrochemical double layer capacitance (C_{dl}) by collecting cyclic voltammograms (CVs) in a non-faradaic region, as ECSA is proportional to the C_{dl} value for the same material. The C_{dl} of the resulting materials was obtained from a series of CV tests conducted at various scan rates (10, 20, 40, 60, 80, and 100 $mV \cdot s^{-1}$) within the potential range of 0.8 to 1.6 V against RHE. By plotting different scan rates against the corresponding current density (j) between the anode and cathode ($j_{anodic} - j_{cathodic}$) at 0.9 V versus RHE, a linear slope was determined as C_{dl}.

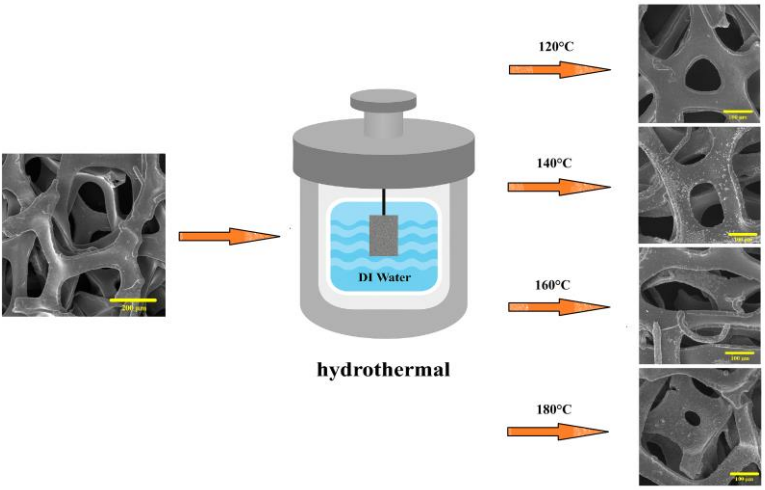

Fig. 1. A schematic illustration of the fabrication procedure by hydrothermal method.

3 Results and Discussion

3.1 Morphological and Chemical Characterization

Fig. 2 displays FESEM micrographs of unaltered Ni foam (NF) alongside samples subjected to hydrothermal treatment at temperatures of 120, 140, 160, and 180 °C. A distinct morphological transformation that depends on temperature is apparent, illustrating the nucleation and growth characteristics of nickel-based hydroxide/oxide phases in hydrothermal environments. The surface morphology of the untreated Ni foam undergoes a distinct, temperature-dependent evolution during hydrothermal treatment, starting as a smooth, featureless surface. At 120 °C, only sparse nucleation sites appear, but a significant transformation occurs at 140 °C, where the surface be-

comes densely covered with plate-like and rod-like microcrystals. This morphology evolves further at 160 °C into a highly porous network of elongated needles and spherical "flower-like" aggregates of nanosheets, maximizing surface area through complex secondary growth. Ultimately, at a temperature of 180 °C, phenomena such as Ostwald ripening led to a conclusive transformation into larger, distinct, and well-defined hexagonal crystals, signifying a transition towards a structure that is less dense yet more thermodynamically stable and crystalline.

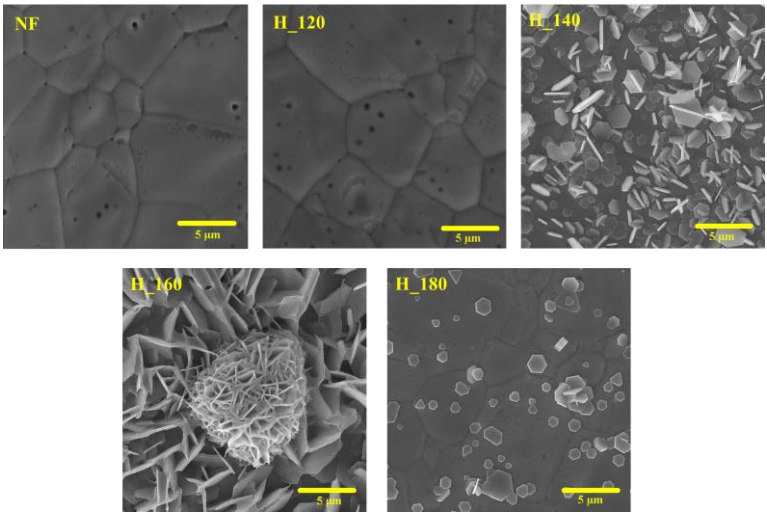

Fig. 2. FE-SEM images of pristine Ni foam (NF) and hydrothermally treated samples at 120°C (H_120), 140°C (H_140), 160°C (H_160), and 180 °C (H_180). All scale bars correspond to 5 µm.

FTIR analysis (Fig. 3) reveals systematic chemical changes on the Ni foam surface corresponding to the increased hydrothermal treatment temperature. While the pristine and 120 °C samples show minimal chemical modification, samples treated at 140 °C and 160 °C exhibit a dramatic intensification of characteristic bands for O–H stretching (3200–3600 cm^{-1}), H–O–H bending (~1600 cm^{-1}), and Ni–O/Ni–OH vibrations (400–600 cm^{-1}). This indicates a significant formation of nickel hydroxide phases with abundant hydroxyl groups and trapped water, which is most pronounced at 160 °C. At 180 °C, the intensity of hydroxyl-related bands decreases while the Ni–O peaks become sharper, signaling partial dehydration and enhanced crystallinity.

Collectively, these spectral trends map a clear, temperature-dependent growth mechanism. The process begins with minimal hydroxylation at 120 °C, transitions to the robust formation of nickel hydroxide at 140 °C, and culminates in a highly developed nanostructured hydroxide layer at 160 °C, consistent with FESEM observations. The final shift at 180 °C confirms a transformation towards more thermodynamically stable, crystalline oxide or oxyhydroxide species. This evolution from a metallic surface

to ordered, crystalline nickel-based nanostructures is thus strongly supported by the vibrational spectroscopy data.

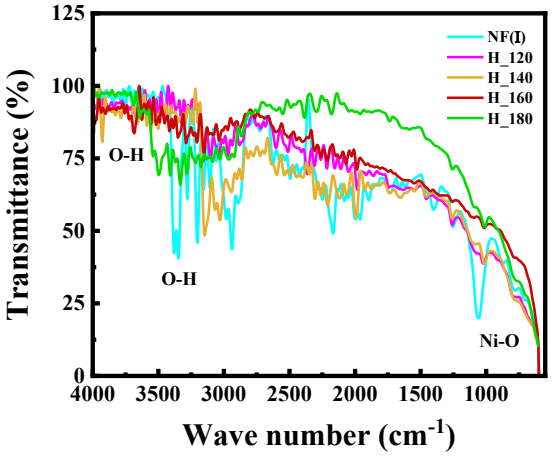

Fig. 3. FTIR spectra of pristine Ni foam (NF) and hydrothermally treated samples at 120, 140, 160, and 180 °C.

3.2 Electrochemical Characterization

The electrochemical behavior of the pristine and hydrothermally treated Ni foam electrodes was first examined using cyclic voltammetry (Fig. 4a). All samples display the characteristic Ni (II)/Ni (III) redox transition, but the magnitude and sharpness of these features depend strongly on the hydrothermal temperature. The pristine Ni foam and the H_120 sample exhibit only weak redox peaks, consistent with their limited surface modification. In contrast, H_140 and especially H_160 electrodes show significantly enhanced redox currents and enlarged enclosed areas, indicating a larger population of electrochemically active sites. The H_160 sample, which develops a high-surface-area flower-like and hierarchical morphology, exhibits the most intense and well-defined redox features. At higher temperature (H_180), redox activity remains stronger than at low temperature but decreases relative to H_160, reflecting the reduced effective surface exposure due to the formation of fewer number of faceted crystals at the surface of H_180 electrode.

To investigate how hydrothermal synthesis temperature affects the surface properties of fabricated thin films, we measured two key parameters: electrochemical double-layer capacitance (C_{dl}) and electrochemical surface area (ECSA). As you can see in Fig. 4b, both C_{dl} and ECSA increased as the synthesis temperature was raised from 120 °C to 160 °C. At 120 °C, the films exhibited the lowest values, indicating a limited number of active sites—likely due to incomplete film formation or insufficient coverage on the nickel foam. When the temperature was increased to 140 °C and 160 °C, both parameters improved significantly, suggesting better surface coverage and the development of more electrochemically accessible nanostructures. The high-

est values were observed at 160 °C, where the films were highly porous and well-adhered which contribute to greater exposure of active sites. The observed correlation between C_{dl} and ECSA across the temperature range underscores the critical role of synthesis temperature in determining the electrochemical performance of these nickel-based catalysts. The substantial increase in both parameters between 140 °C and 160 °C suggests a temperature-driven transition in the film's microstructure and composition. These enhancements in surface characteristics directly contribute to improved OER performance at higher synthesis temperatures up to 160 °C. However, if the temperature exceeds 180 °C, the surface area may plateau or even decrease, potentially due to film densification or overgrowth, which could limit electrolyte access. Overall, these findings indicate that 160 °C is the optimal hydrothermal temperature for maximizing active site density and charge storage capacity in $Ni(OH)_2/NiOOH$ thin film electrodes for water splitting. Moreover, the catalytic activity toward the anodic reaction was evaluated using linear sweep voltammetry (Fig. 4c).

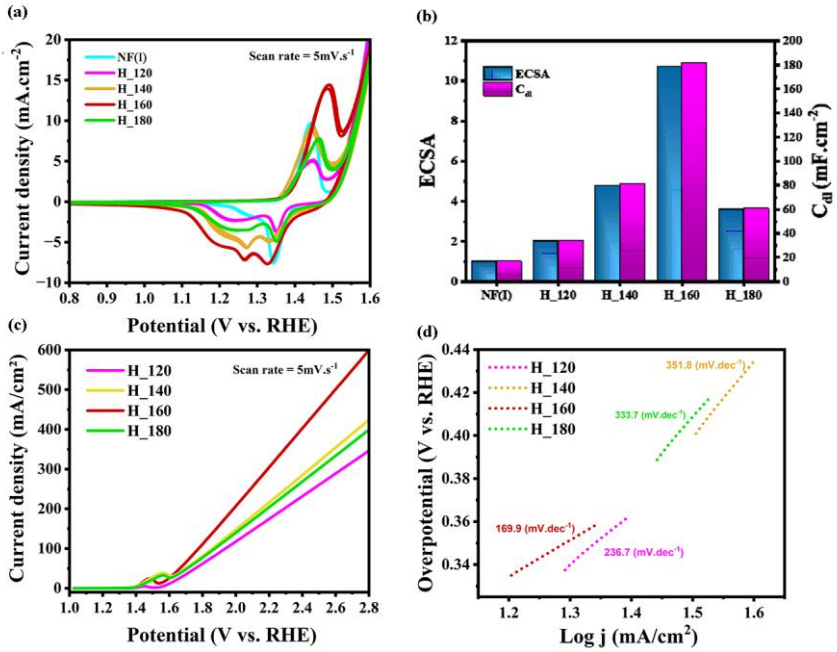

Fig. 4. (a) The cyclic voltammetry curves at a scan rate of 5 mV/s, (b) electrochemical surface area (ECSA) and double-layer capacitance (C_{dl}), (c) linear sweep voltammetry curves at a scan rate of 5 mV/s, and (d) Tafel plots and corresponding slopes of pristine Ni foam (NF) and hydrothermally treated samples at 120, 140, 160, and 180 °C.

The H_160 electrode delivers the highest current density and the lowest onset overpotential (0.31V), demonstrating the most efficient charge transfer and oxygen-evolution behavior. Both H_140 and H_180 samples show intermediate performance with the

overpotential of (0.39V) and (0.38V), respectively, whereas H_120 exhibits relatively poor catalytic activity.

Kinetic analysis through Tafel fitting (Fig. 4d) further confirms the superior catalytic behavior of the H_160 sample. With the lowest Tafel slope (≈170 $mV \cdot dec^{-1}$), H_160 demonstrates more favorable reaction kinetics than all other electrodes, requiring a smaller increase in overpotential to achieve a tenfold increase in current. The H_120, H_140, and H_180 samples show substantially higher Tafel slopes, indicative of slower charge-transfer kinetics and less optimal surface energetics for the OER. These observations align directly with the structural and chemical evolution revealed in FE-SEM and FTIR analyses: only at 160 °C does the hydrothermal process yield a synergistic combination of high surface area, abundant hydroxide/oxyhydroxide species, and hierarchical porosity, all of which contribute to enhanced intrinsic and geometric catalytic performance. These results reflect a combined effect of surface area, chemical state, and morphology: the highly porous framework of H_160 promotes rapid electrolyte penetration and efficient mass transport, while the abundant Ni–OH/NiOOH sites revealed by CV and FTIR provide a favorable surface for OER intermediates. In contrast, the smaller, more separated crystalline structures appearing at 180 °C reduce the density of active sites, leading to diminished LSV performance relative to H_160 alongside higher overpotential.

4 Conclusion

The influence of hydrothermal synthesis temperature on $Ni(OH)_2$/NiOOH thin films grown on nickel foam was systematically investigated for the alkaline oxygen evolution reaction (OER), revealing a clear temperature-dependent evolution in the material's structure and catalytic activity. Structural and chemical analyses confirmed that increasing the temperature promoted a morphological transition from sparse nucleation (120 °C) to dense hydroxide nanostructures (140 °C), culminating in a highly porous, hierarchical network of nanosheets at 160 °C, before transforming into less active, larger crystalline domains at 180 °C. Crucially, these structural changes directly correlated with electrochemical performance, with the 160 °C sample exhibiting superior OER activity, evidenced by the lowest overpotential, smallest Tafel slope, and the highest electrochemical surface area. This optimal performance is attributed to a synergistic combination of abundant active sites within a highly accessible nanostructure, establishing 160 °C as the ideal synthesis temperature and highlighting a simple, effective route for rationally designing high-performance, scalable electrocatalysts for alkaline water splitting.

Acknowledgments. The authors thank Pasargad Institute for Advanced Innovative Solutions (PIAIS) for financial support of project number 10202.

Disclosure of Interests. The authors have no competing interests to declare that are relevant to the content of this article.

References

1. Roger, I.; et al. Electrochemical water splitting: A review of electrode materials and catalysts. *Chem. Soc. Rev*. 2017, 46, 1780–1803.
2. Seh, Z. W.; et al. Combining theory and experiment in electrocatalysis: Insights into materials design. *Science* 2017, 355, eaad4998.
3. Koper, M. T. M. Thermodynamic theory of multi-electron transfer reactions: Implications for electrocatalysis. *J. Electroanal. Chem*. 2011, 660, 254–260.
4. Zhang, J.; et al. Oxygen electrocatalysis in alkaline media: From fundamentals to applications. *Energy Environ. Sci*. 2020, 13, 3361–3392.
5. Song, F.; Hu, X. Exfoliation of layered double hydroxides for enhanced oxygen evolution catalysis. *Nat. Commun*. 2014, 5, 4477.
6. Xu, X.; et al. Engineering $Ni(OH)_2$ into NiOOH via electrochemical activation: Phase evolution and OER activity. *ACS Appl. Mater. Interfaces* 2020, 12, 34748–34757.
7. Louie, M. W.; Bell, A. T. An investigation of thin-film Ni–Fe oxide catalysts for the oxygen evolution reaction. *J. Am. Chem. Soc*. 2013, 135, 12329–12337.
8. Dionigi, F.; et al. In situ structure and catalytic mechanism of NiFe and CoFe layered double hydroxides during oxygen evolution. *Nat. Commun*. 2020, 11, 2522.
9. Zhang, Y.; et al. Hierarchically porous Ni foam as an efficient scaffold for hybrid water-splitting catalysts. *ACS Appl. Energy Mater*. 2021, 4, 1256–1265.
10. Yu, F.; et al. Fe-doped $Ni(OH)_2$ nanosheets with improved OER performance. *ACS Catal*. 2019, 9, 9973–9981.
11. Jin, H.; et al. Ni–Mo–S nanosheets grown on Ni foam for efficient OER. *Energy Environ. Sci*. 2016, 9, 3371–3378.
12. Wang, Y.; et al. Effect of synthesis temperature on the morphology and electrocatalytic activity of $Ni(OH)_2$/NiOOH films. *Electrochim. Acta* 2019, 306, 437–445.
13. Jiang, N.; et al. Nickel hydroxide nanosheets with temperature-dependent OER activity. *J. Mater. Chem. A* 2020, 8, 25317–25325.
14. Pour-Ali, S.; et al. Enhanced photoelectrochemical water splitting via hydrogenated TiO2 nanotubes modified with Cu/CuO species. *J. Photochem. Photobiol., A* 2024, 452, 115586.